FE-Analysis of Stringer-to-floor-beam Connections in Riveted Railway Bridges

By Mohammad Al-Emrani[1] and Robert Kliger[2]
Department of Structural Engineering
Chalmers University of Technology, SE-412 96 Göteborg, Sweden

Abstract: Stringer-to-floor-beam connections in riveted railway bridges have in many cases shown to be critical details with respect to fatigue. These connections, while generally designed with respect to shear forces alone, are often subjected to repeated out-of-plane distortion as a result of their rotational stiffness. The behavior of double-angle stringer-to-floor-beam connections in riveted railway bridges is examined using finite element analysis. A series of static and fatigue tests was performed on three full-scale bridge parts taken from an old riveted railway bridge in order to study the response of these connections under the action of bending moment. The results of the analysis show that these double-angle "shear" connections are capable of developing appreciable moment due to the restraint they exert on the rotation of stringer ends associated with bending. The resulting bending and axial stresses in the angles and the rivets of the connection might consequently be considerable. High stress concentrations are also present in these components, which further increases their fatigue-damage susceptibility.

Keywords: Railway bridges, riveted connections, stringer-to-floor-beam connections, fatigue.

1. INTRODUCTION

The floor-system in old riveted railway truss bridges is typically designed as a grid structure consisting of longitudinal and transverse members (stringers and floor-beams) connected through their web plates by means of riveted double-angles. The main function of these connections is to transfer the stringer end reactions to the floor-beams through shear action.

One general assumption that is made in the design of these double-angle connections is that they have sufficient rotational flexibility to allow for the stringer-end rotation associated with bending without developing appreciable moment. This assumption is also often adopted today. Analyses of the load-carrying capacity of double-angle stringer-to-floor-beam connections in existing riveted bridges, and the assessment of their fatigue strength, are generally made with reference to the shear forces acting on the connections only.

The assumption of null degree-of-fixity might be justifiable when it comes to the ultimate load-carrying capacity of the connections and the connected members. However, overlooking the effect of the rotational stiffness of these connections might result in an inadequate estimation of their fatigue strength.

---

[1] Corresponding author, graduate student, Tel. +46 772 22 58; E-mail: mohammad.alemrani@ste.chalmers.se
[2] Professor; Steel and Timber Structures.

A relatively large number of fatigue-damage cases in double-angle stringer-to-floor-beam connections have been reported, the majority of which were attributed to the moment acting on these connections [1], [2], [3].

As part of an investigation on the fatigue performance of riveted stringer-to-floor-beam connections, a series of static and fatigue tests was performed on three full-scale bridge parts taken from an old riveted railway bridge. Strain and deformation measurements were made in connection with the static tests in order to monitor the response of the specimens at various load levels. The results of these measurements were used to verify a finite element analysis of the tested specimens, which is the primary concern of this paper.

Finite element analyses of mechanically-fastened connections have been carried out extensively and in various forms over the years. Depending on the level of the structural analysis and the type of results sought, these models vary in the degree of complexity, from simple plane models with essentially 1-D elements (beam, spring, rigid and gap elements) to space models with shell and/or solid elements. Generally, the problem involves a number of complexities, such as material and geometric non-linearities and contact-separation modeling. The work performed in this field has been primarily concerned with the ultimate load-carrying capacity of bolted connections under both static and seismic loads. In particular, beam-column and column-base connections have been widely studied. Nevertheless, experience acquired in this field is generally also applicable to other types of mechanically-fastened connections. Benchmarks and recommendations on the choice of suitable element type, appropriate discretization and modeling of the contact-separation problem have been presented by several researchers in this field [4], [5], [6].

The primary objectives of the FE-analysis conducted on the tested specimens are to closely examine the performance of the stringer-to-floor-beam connections in these specimens and to obtain, on the basis of the static tests performed, a complementary picture of their behavior. In particular, the load-deformation characteristics of the connections and the nature and magnitude of stresses resulting in the different components are studied. The effect of clamping force in the rivets on the response of the connections is also examined.

2. LABORATORY TESTS ON FULL-SCALE BRIDGE PARTS

Three full-scale bridge parts were taken from the old riveted railway bridge over the river Vindelälven in northern Sweden. The bridge, which was built in 1896 and demolished in 1993, had three simply-supported arch-shaped truss spans of 71.2 m each. The floor system in each span consisted of 13 floor beams connected to two rows of stringers (2x12 stringers). Each test specimen consisted of three floor beams and four stringers connected to each other with riveted double angles. Fig. 1 shows the set-up of the test specimens and loading arrangement, together with a detail of the double-angle connections.

The specimens were supported at three pairs of bearing points, each positioned under a floor beam where the stringers meet the floor beams. The load was provided by four hydraulic jacks, each placed at the center line of a stringer. The force provided by each

hydraulic jack was then transferred to the stringer as two point loads via a distribution beam, which resulted in each stringer being loaded in four-point bending.
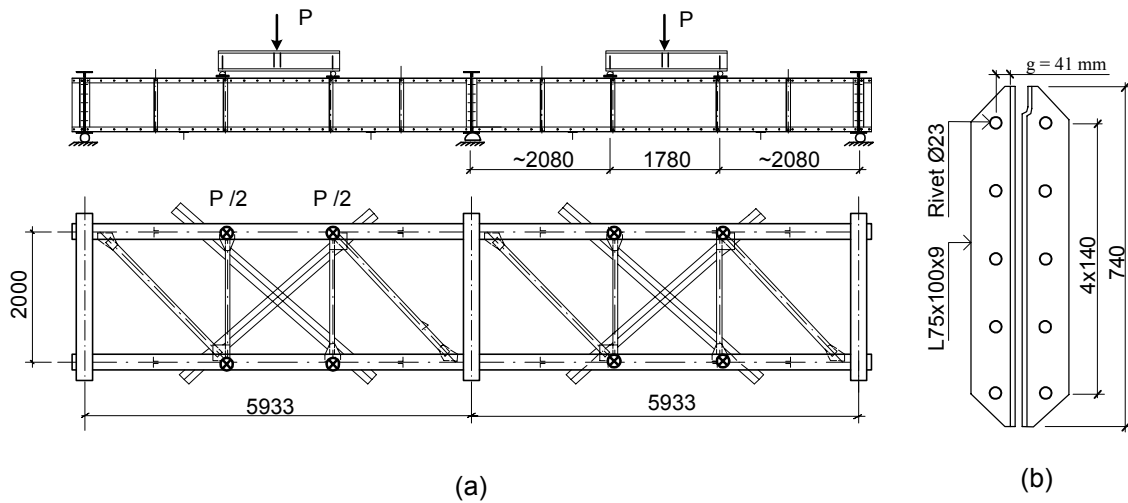

(a)   (b)

Fig.1 The riveted bridge parts that were tested: (a) test set-up; (b) detail of the connections.

3. FINITE ELEMENT ANALYSIS

3.1 Description of the model

The finite element model adopted for the analysis of the specimens tested here is shown in Fig. 2. Symmetry is assumed with respect to two perpendicular planes passing through the center lines of both the central floor beam (plane XZ) and the stringer (plane YZ). Together with the symmetry of the applied load, this allowed the model to be limited to half a stringer and one connection angle with its corresponding rivets.
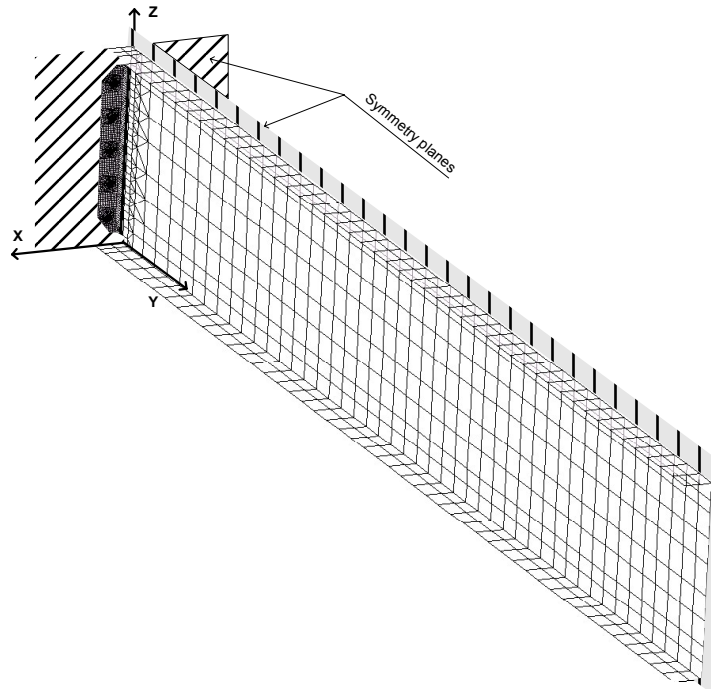

Fig. 2. The finite element model adopted for the analysis of the tested specimens.

Some simplifications and assumptions also had to be adopted in order to facilitate the building of the FE model, reduce the calculation costs and ease the post-processing of the results:

- Nominal dimensions, as stated in the technical drawings of the bridge, were adopted in the model, although some deviation from these dimensions could be noted (e.g. rivet center and gauge distances).

- The rivets in the model were given an initially "perfect" shape. This was not the case for all the rivets in the actual connections. A wide range of variation in rivet shape and dimensions was observed, with many rivets having "flattened" and/or eccentrically shaped rivet heads.

- Tension tests, previously performed on coupon specimens taken from stringer flanges and some rivets in stringer-flange connections [7], were used to define the stress-strain relations for the steel in the angles and the rivets respectively, see Fig. 3.
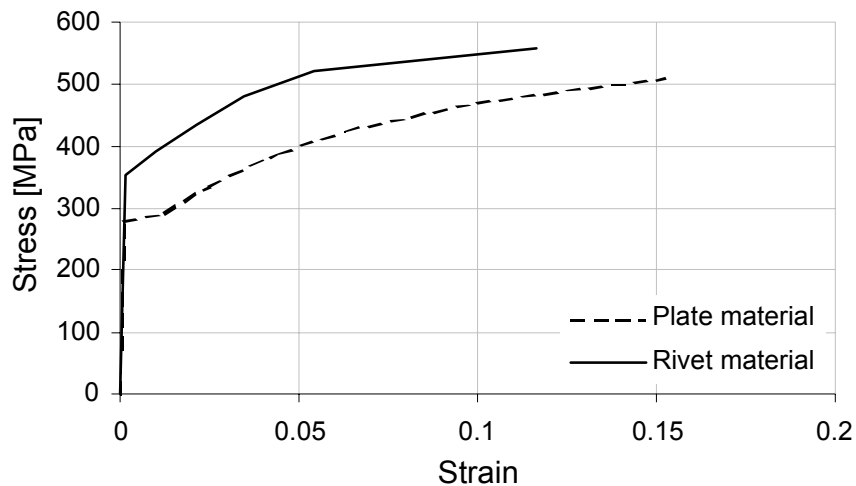

Fig. 3. Stress-strain relations adopted for the rivet and plate material in the FE-model.

In the first step, a discretization study with three different mesh densities was performed. Solid elements were used for the angle and the rivets in the connection, while the stringer was meshed using shell elements. Furthermore, two different element types were also examined for the solid elements in the connection. These were either 8-node or 20-node brick elements. Fig. 4 shows two examples of the models examined in this study.

Contact between the back-face of the outstanding leg of the connection angle and the floor-beam web was simulated by means of a rigid contact surface, meshed with linear quadratic rigid elements (R3D4). A classical Coulomb-friction model, with a friction coefficient ($\mu =$ 0.3) was used in all the contact pairs in the model (rivet-to-connection angle and connection angle-to-rigid surface). All models were generated using I-Deas Master Series 8 and the analysis was then performed with the commercial FE-package ABAQUS 5.8.
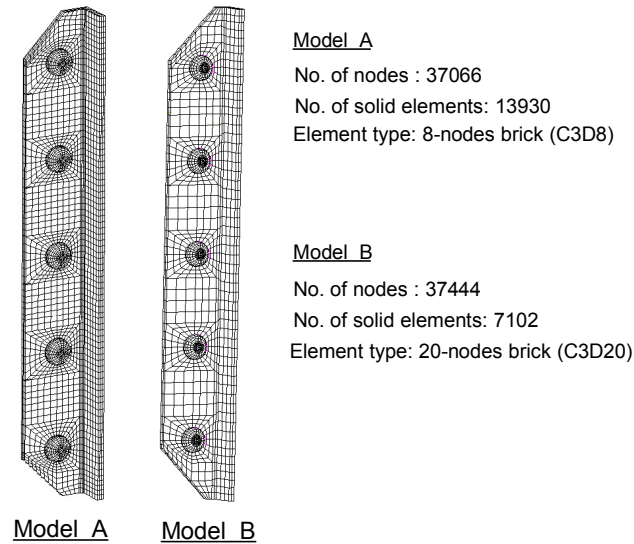
Model A

No. of nodes : 37066
No. of solid elements: 13930
Element type: 8-nodes brick (C3D8)

Model B

No. of nodes : 37444
No. of solid elements: 7102
Element type: 20-nodes brick (C3D20)

Model A   Model B

Fig. 4. Two examples of the models examined in the discretization and element-type studies.

3.2 Verification of the model

Two main criteria were adopted to verify the FE-models in view of the results obtained from the static tests. Firstly, the ability of the model to "reproduce" the correct stiffness of the connection was checked against displacement and strain measurements made at the top of the connection angles and at the mid-span of the stringers respectively (the results are discussed in detail later on in the next section). Secondly, strain gauges installed at different locations along the stringer depth near the connection were used to register the distribution of local stresses in these locations. The measured values were compared with the corresponding values obtained from the FE-analysis and an example of the results is shown in Fig. 5.

One (initially unknown) variable that might affect the response of the connections is the magnitude of the clamping force in the rivets. The analysis was therefore performed with three different rivet pre-tension values (30, 65, and 140 MPa) and the results are compared with and related to strain measurements made on one of the rivets in the connections.

Local flexural strains near the fillet of the connection angles were also measured during the static tests, at different locations along the depth of several connections (1 mm long strain gauges were used for this purpose). Although the stresses in locations of stress concentration of this type are fairly sensitive to the position of the strain gauges, the results of these measurements are used as a "general reference" to the ability of the model to reflect the bending characteristics of the connection angles.

Both models shown in Fig. 4 were capable of reflecting the load-deformation characteristics of the connection and the results obtained showed a good correlation (in terms of stress and stiffness) to the reference values obtained from the static tests. Model A, with C3D8-elements was, however, more cost effective and was therefore adopted for the analysis.
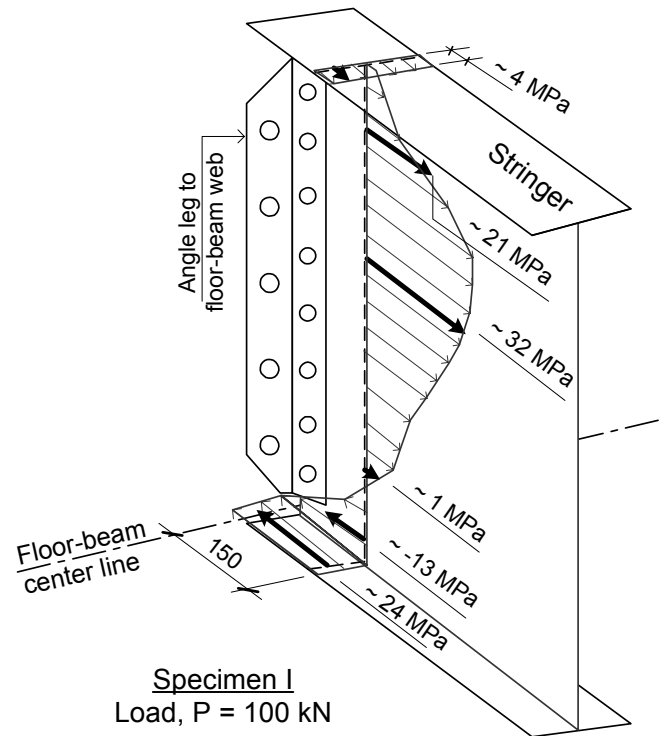

Fig. 5. Measured and calculated bending stresses in the stringer near the connection.

4. RESULTS OF THE FE-ANALYSIS

4.1 The Behavior of Riveted Double-angle Connections Subjected to Moment

The rotational stiffness of double-angle stringer-to-floor-beam connections is primarily a function of the flexural stiffness of the outstanding legs of the connection angles. The effect of the deformation applied to the connections (by the stringer-end rotation associated with bending) is to subject the outstanding legs in the upper portion of the connection to an out-of-plane flexure, causing bending and axial stresses in the angles and the rivets respectively. The magnitude of stringer-end moment and the resulting forces in the different components of the connection will depend on the amount of applied deformation that can be accommodated by the flexural flexibility of the outstanding legs.

Fig. 6(a) shows the deformed shape of the connection part considered in the FE-analysis. The out-of-plane distortion of the outstanding leg along the depth of the connection is also shown in Fig. 6(b). The magnitude of deformation involved in the response of the connection is extremely small. This was also confirmed by displacement measurements made on the top of two opposite connection angles during the static test of one specimen. The measured out-of-plane distortion of the outstanding leg (relative to the floor-beam web) is shown in Fig. 6(c), along with the corresponding values obtained from the FE-analysis for three different rivet-clamping stresses.
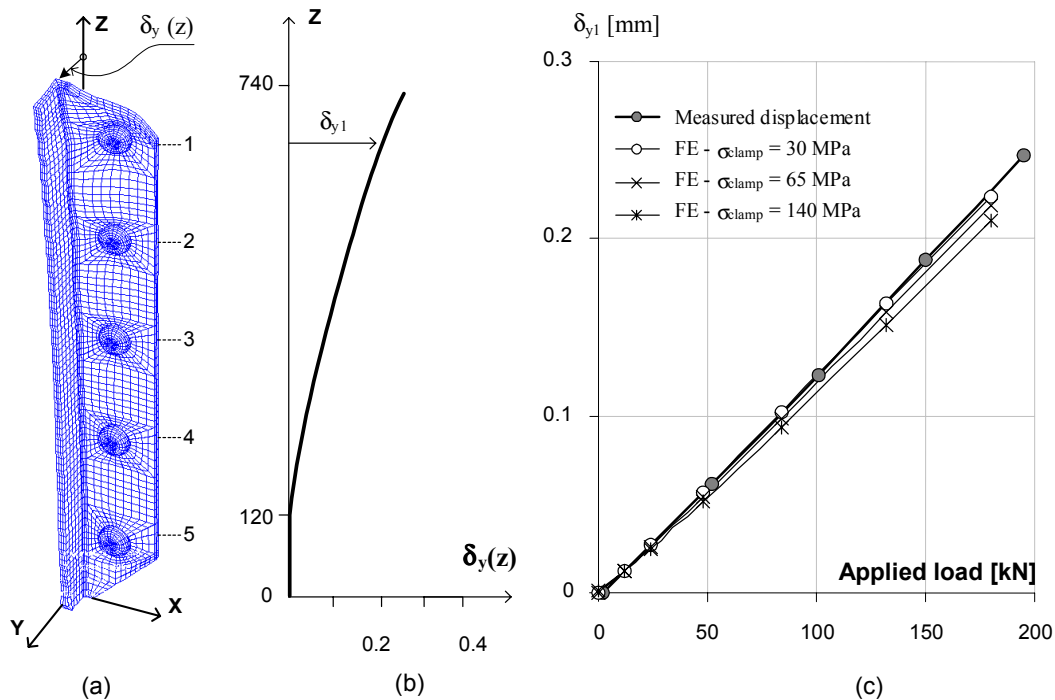

Fig. 6. Out-of-plane distortion of a connection angle: (a) deformed shape of the connection; (b) the out-of-plane displacement along the depth of the angle (P = 180 kN); (c) measured and calculated displacement at the top of the connection.

A large part of the deformation applied to the connection by the rotation of the stringer end is "locked" by the stiffness of the connection. Consequently, the angle is subjected along most of its depth to tensile forces which are counterbalanced by local contact pressure at the bottom of the connection, see Fig. 7. If the connection is regarded as a series of mutually-independent angle segments with depth C, the axial forces acting on the connection can be calculated on the basis of the axial stress in the angle leg connected to the stringer web (σ_y). The upper part of the connection is subjected to relatively high tensile forces and the magnitude of stringer-end moment is considerable. The double-angle "shear" connections were capable of developing more than 60% of the corresponding moment for a totally rigid connection! The moment-load behavior for the load range studied here was essentially linear and the position of the rotational center was only slightly affected by the magnitude of the applied load.
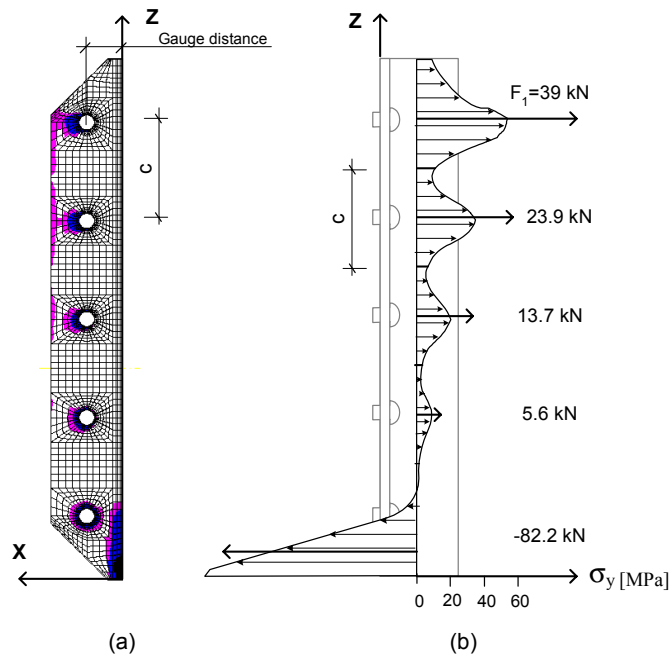
Fig. 7. The forces acting on the connection due to the action of moment: (a) contact pressure on the back side of the outstanding leg; (b) axial forces and stresses in the angle leg connected to the stringer web (P = 180 kN).

4.2 Load-deformation Characteristics of the Connection Angles

As has already been stated, the flexibility of the outstanding legs of double-angle connections subjected to moment has a major impact on the response of these connections. In particular, the gauge distance between the rivets and the fillet of the angle plays a dominant role in the behavior of these connections. On the one hand, the flexibility of the outstanding leg at these locations has a decisive effect on the amount of applied deformation that can be accommodated by the connection and, consequently, on the magnitude of the stringer-end moment. Furthermore, due to its locally higher stiffness, the outstanding leg along the gauge distance attracts a larger portion of the tensile forces acting on the connection, resulting in high stress concentration at these locations. The bending stresses in the outstanding leg of the angle are mostly magnified along the gauge length and reach a maximum near the fillet of the angle, see Fig. 8(a). In fact, an examination of the equivalent Von Mises stresses at the fillet of the angle near the upper rivet reveals that the connection angles in the tested specimens might have experienced plastic strains at these locations, but to a very limited extent. The stresses in the rivets were, however, fully elastic.

When the distribution of stresses in the angle shown in Fig. 8 is analyzed, a number of observations can be put forward. Although the behavior of the outstanding leg of the angle is bending dominated, some "membrane action" appears to exist. Based on the distribution of stresses through the thickness of the angle near the fillet, the contribution from the membrane action in this location is less than 10% of the bending stresses.
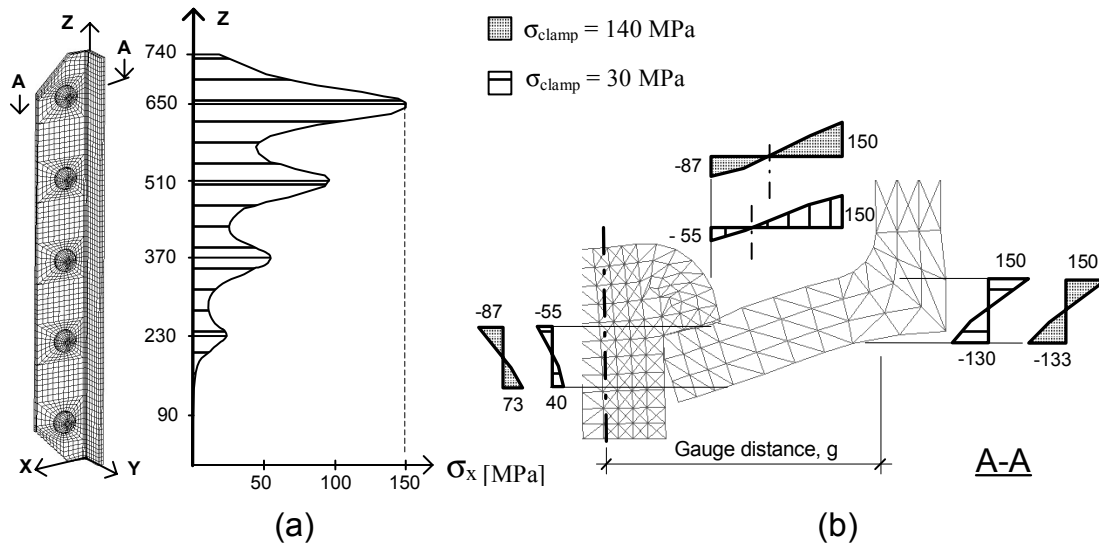
Fig. 8. The distribution of bending stresses in the connection angle (P=100 kN): (a) near the fillet along the depth of the connection; (b) along the gauge distance and through the thickness of the angle.

The rivet clamping force had a negligible effect on the magnitude of maximum bending stresses near the fillet of the angle. On the other hand, higher bending stresses were produced in the outstanding leg near the rivet when the latter had a higher clamping force. The outstanding leg of the connection angle behaves as though it was partially fixed under the rivet head. With a higher clamping force, the outstanding leg approaches the fixed-end beam model presented by Wilson and Coombe in 1939 [8], where it is regarded as totally fixed along the rivet center line and the fillet of the angle. The same behavior explains the slightly stiffer response obtained for the connections with a higher rivet-clamping force (cf. Fig. 6). The deformation of the outstanding leg near the rivet is restricted by the axial and bending stiffness of the latter and is consequently affected by its clamping force. The separation of the back side of the outstanding leg under the rivet head from the rigid surface occurred at different load levels for different values of rivet-clamping stress (P = 30, 80 and 170 kN for σ_{clamp} = 30, 65, and 140 MPa). The axial stiffness of the rivets is typically several times greater than the flexural stiffness of the outstanding leg of the angle and the contribution from rivet elongation to the flexibility of the connection is relatively small.

One clear observation regarding the distribution of "bending" stresses along the depth of the connection (Fig. 8(a)) is that the outstanding leg of the angle is not equally active in resisting the applied deformation (or the resulting tensile forces). The locally stiffer part of the outstanding leg at the rivet gauge distance attracts a larger percentage of these forces. If, once again, the connection angle is regarded as a number of mutually-independent L-segments with depth C, an equivalent effective depth, C_{eff}, can be calculated for each segment on the basis of the bending stresses, $\sigma_x(z)$. The bending moment (per unit length) along the depth of the segment is:

III-9

$$M_z(z) = \sigma_x(z) \cdot \frac{t^2}{6} \qquad (1)$$

where $\sigma_x(z)$ and t are defined in Fig. 9. The resulting total moment acting on the outstanding leg of the segment can be obtained as:

$$M_z^{tot} = \int_0^c M_z(z)dz \qquad (2)$$

The depth of the assumed effective segment, with an equivalent maximum bending moment, M_z^{max} could thus now be calculated as:
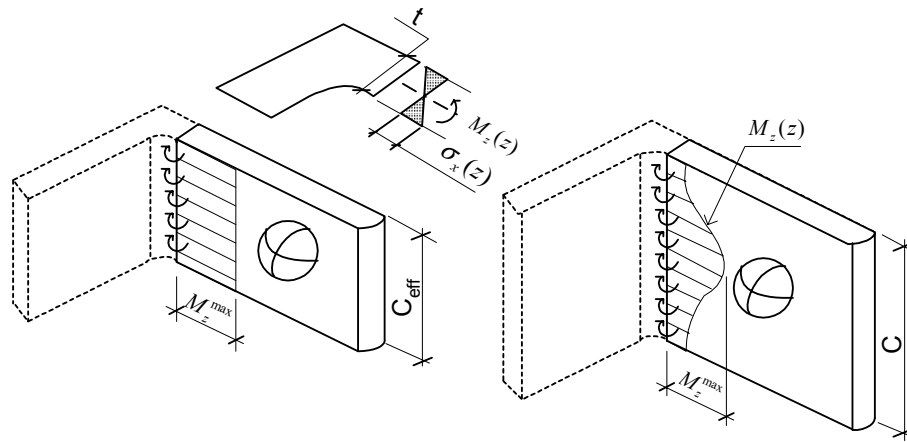
$$C_{eff} = \frac{M_z^{tot}}{M_z^{max}} \qquad (3)$$

Fig. 9. Calculation of the effective width of an equivalent L-segment in the connection.

The value of $Ceff$ was calculated for the four segments in tension in the connection at various load levels and was found to be around 90 mm for all segments, irrespective of the load level that was considered.

The equivalent L-steel segment also reflected the stiffness of the connection reasonably well. The axial displacements of the four upper segments of the connection under tension were calculated using the axial segmental forces (F_i in Fig. 7) and the fixed-end beam model, proposed by Wilson and Coombe [8]. The calculated values are shown in Fig. 10, together with the deflection curves of the angle obtained from the FE-analysis, for two different load levels. As expected, the fixed-end model overestimates the stiffness of the angle segment somewhat by assuming that the outstanding leg is fully fixed at the rivet. A further overestimation of the stiffness would be obtained if the full actual depth, C, was used for the presumed L-segment.
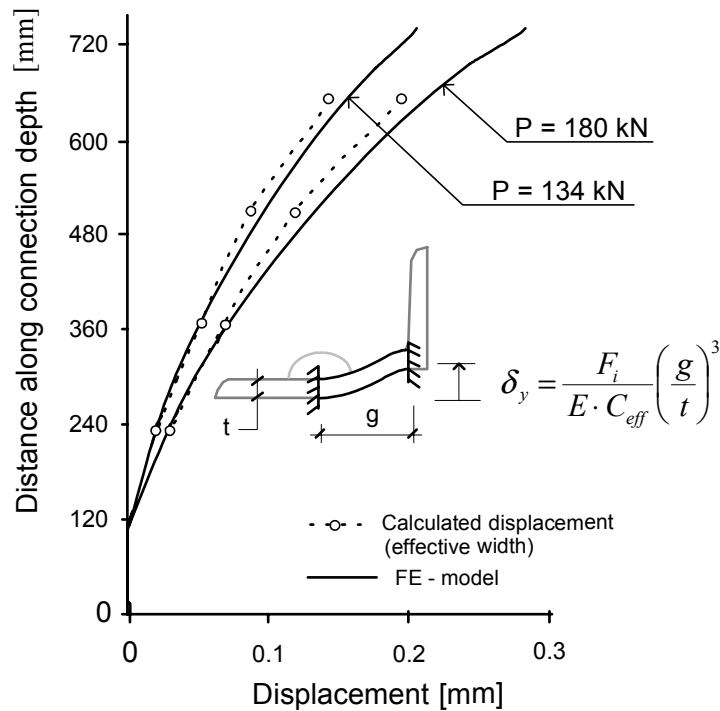
Fig. 10. Out-of-plane distortion of the connection angles (FE-model), and the corresponding displacement of the equivalent L-segments with an effective width, Ceff.

4.3 Axial and Bending Stresses in the Rivets of the Connection

It is well known that the clamping force in the fasteners of connections subjected to fluctuating moment and/or tensile forces has a significant influence on the fatigue strength of these fasteners. For a given applied load, a higher clamping force will simply result in a smaller increase in the axial force developed in these fasteners.

Several previous investigations relating to riveted connections have concluded that hot-driven rivets could develop considerable clamping forces. In 1938, Wilson and Thomas [9] performed a series of tests in which the initial clamping force in the rivets was measured. The average clamping ratio (i.e. the ratio between the clamping stress in the rivet and the rivet yield stress) was found to be about 70%. The clamping force in the rivets of flange-to-web connections was investigated by Åkesson [7] for stringers taken from the same bridge that was studied in this investigation. The average value of the clamping ratio found in these rivets was 42%.

Generally, the clamping force in hot-driven rivets is a highly undetermined variable. In addition to its dependence on the grip length (i.e. shank) of the rivet and the stiffness of the connected plates, it is also affected by the driving temperature, the driving method (e.g. hand-hammering or using hydraulic-pressure riveters). The magnitude of the clamping force is also expected to be reduced with time through relaxation or due to the fretting of the connected components.

In particular, the rivets in stringer-to-floor-beam connections are expected to have substantially lower clamping stress. These connections are generally assembled on site, which often involves uncontrolled riveting conditions and installation problems which could result in faulty, misshapen rivets (a large number of rivets with flattened and/or eccentric rivet heads could actually be observed in the tested specimens).

In order to obtain information about the magnitude of the stress range expected to be present in the rivets during fatigue loading of the tested specimens, strain measurements were made on an upper rivet in one of the connections using a strain gauge specially designed for uniaxial strain measurements in bolts. Although the measured nominal tensile stresses represent only the average increase in rivet force at different load levels, an estimation of the initial clamping stress in this rivet can also be obtained by comparing the nominal tensile stresses obtained from the FE-analyses using different rivet clamping stresses with the measured values (superimposed by the same presumed initial clamping stresses), see Fig. 11. A good correlation was obtained between measured and calculated axial stresses for the model with a rivet clamping stress of 30 MPa. This was also in agreement with the results relating to the out-of-plane deformation of the angles at the top of the connection (cf. Fig. 6).

The positive effect of the rivet-clamping force on the variation in axial stress in the rivet can be clearly seen in Fig. 11. Increasing the initial clamping stress from 30 to 140 MPa reduced the total stress range (for a zero-to-maximum load range) by about 60%.
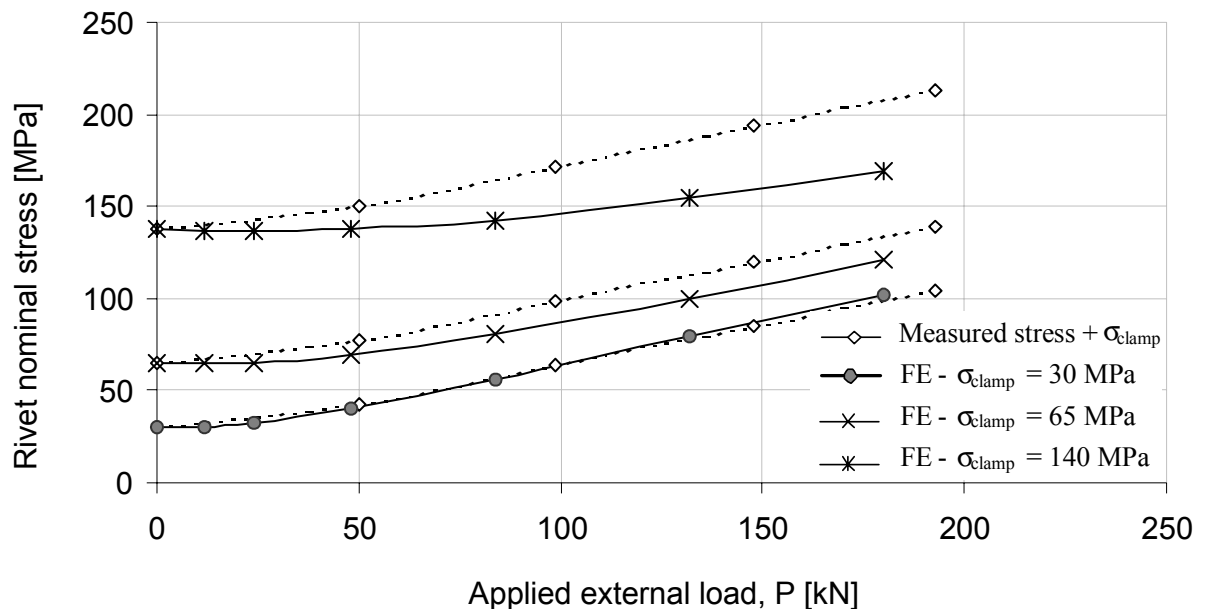

Fig. 11. Measured and calculated nominal axial stress in the upper rivet of the connection.

The effect of the clamping force in the rivets on their fatigue strength is even more pronounced when taking account of the variation in local stresses in the rivet shank, where the effect of rivet bending is also included, see Fig. 12. In fact, the bending of the rivets caused by the flexure of the outstanding legs of the connection angles, together with the stress concentration present at the junction between the rivet shank and its head, are the major mechanisms behind crack initiation and fracture in these rivets (rather than the variation in the nominal axial tensile stress in these rivets).
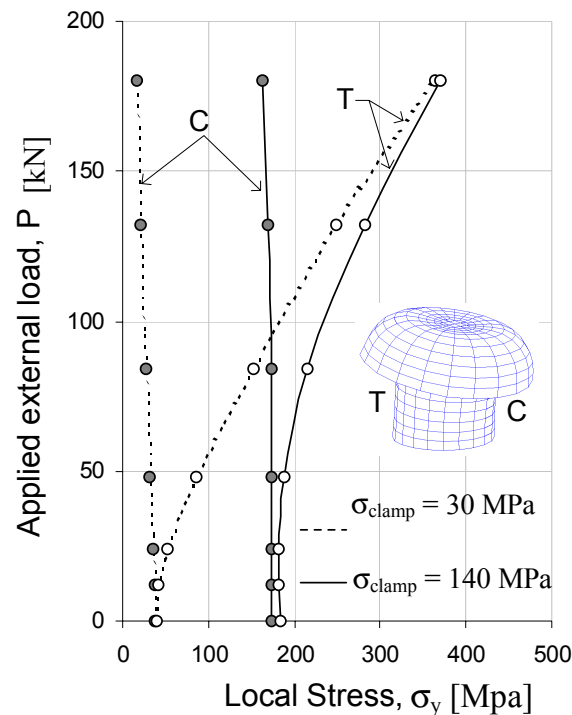

Fig. 12. Local stresses in the rivet shank caused by axial force and bending.

Even though, the magnitude of tensile stresses at maximum load (P = 180 kN) was near the yield stress of the rivet material, the stress range in this location is highly reduced when higher clamping force is present. This reduction decreases, however, with increasing mean-load values. The large variation in tensile stresses (i.e. stress range) near the junction between the rivet shank and its head explains the rather early fatigue failures which were observed for these rivets during the fatigue tests. For the applied load range (P_{min} and P_{max} are 80 and 180 kN respectively), the maximum tensile stress range in the rivet, obtained from the FE-analysis, was about 210 MPa, see Fig. 12.

The rivet in the second row of the connection (looking from the top) also experiences relatively high axial and bending stresses. The "segmental" tensile forces carried by this rivet were also high and were further magnified by the effect of prying (cf. Fig. 7). Fatigue failure in the upper two rivets took place in many of the connections during the fatigue tests of the three bridge parts.

5. SUMMARY AND CONCLUSIONS

Double-angle stringer-to-floor-beam connections have been a common source of fatigue damage in riveted railway bridges. In many cases, this damage is generated by the secondary stringer-end moment that develops at the connections as a result of their rotational stiffness.

The behavior of double-angle stringer-to-floor-beam connections was studied using FE-analysis. Static and fatigue tests were also performed on three full-scale bridge parts taken from an old riveted railway bridge. The results of the analysis show that double-angle stringer-to-floor-beam connections, although generally assumed to act as "simple" shear joints, exert appreciable restraint on the stringer-end rotation associated with bending and, as a result, high secondary bending moment might develop at these connections.

The flexibility of the outstanding legs of the connection angles has a major influence on the response of the double-angle connections. In particular, the gauge distance between the rivets and the fillet of the angle was found to play a dominant role in the behavior of these connections. The outstanding legs of the connection angles were subjected by the action of moment to out-of-plane distortion, which in turn generated high flexural stresses in the angles. The distribution of these flexural stresses along the depth of the connection was, however, not uniform. High concentrations of flexural stresses were present near the fillet of the angle at the rivet gauge distances.

The magnitude of the clamping force in the rivets had only a marginal effect on the rotational stiffness of the connections and the flexural stresses in the angles were virtually not affected by the rivet clamping force. On the other hand, the resulting stress ranges in the rivets of the connection were greatly influenced by the magnitude of clamping force in these rivets. The variation in both axial and bending stresses in the rivets was substantially reduced when a higher clamping force was present.
Rivet bending due to prying action, together with the stress concentration present at the junction between the rivet shank and its head, was found to be the major mechanism behind fatigue cracking in the rivets rather than the variation in the nominal axial tensile stress in these rivets.

References

[1] Aboulmaaty, W. M., Experimental Fatigue Evaluation of Steel Double-angle Connections in Railway Bridges. Master's thesis, University of Nevada, Reno, 1997.

[2] Al-Emrani, M., Two Fatigue-related Problems in Riveted Railway Bridges. Licentiate thesis, Chalmers University of Technology, Department of Structural Engineering, Göteborg, Sweden, 2000.

[3] Wang, D., Fatigue Behaviour of Mechanically Fastened Double-angle Shear Connections in Steel Bridges. PhD thesis, Lehigh University, Pennsylvania, 1990.

[4] Bursi, O. S. and Jaspart, J. P., Benchmarks for Finite Element Modelling of Bolted Steel Connections. Journal of Constructional Steel Research, 43, 17-42, 1997.

[5] Bursi, O. S. and Jaspart, J. P., Calibration of Finite Element Model for Isolated Bolted End-Plate Steel Connections. Journal of Constructional Steel Research, 44, 225-262, 1997.

[6] COST/C1 Action, Control of the Semi-rigid Behaviour of Civil Engineering Structural Connections. European Cooperation in the Field of Scientific and Technical Research - Final Report, Luxembourg, 2000.

[7] Åkesson, B., Fatigue Life of Riveted Railway Bridges. Doctoral thesis, Department of Structural Engineering, Chalmers University of Technology, Göteborg, Sweden, 1994.

[8] Wilson, W. M. and Coombe, J. V., Fatigue Tests on Connection Angles. University of Illinois, Engineering Experiment Station, Bulletin No. 317, Urbana, 1939.

[9] Wilson, W. M. and Thomas, F. P., Fatigue Tests on Riveted Joints. University of Illinois, Engineering Experiment Station, Bulletin No. 302, Urbana, 1938.

Notations

C	Rivet central distance
C_{eff}	Effective width of L-segment
E	Modulus of elasticity
F	Axial force
g	Rivet gauge distance
M	Bending moment
P	Applied load
Pr	Load range
t	Thickness of connection angle
δ	Out-of-plane displacement
σ	Stress
μ	Friction coefficient